

Magnetic susceptibility study of hydrated and non-hydrated $\text{Na}_x\text{CoO}_2\cdot y\text{H}_2\text{O}$ single crystals

F. C. Chou¹, J. H. Cho^{1,2,*} and Y. S. Lee^{1,2}

¹Center for Materials Science and Engineering,
Massachusetts Institute of Technology
and

²Department of Physics, Massachusetts Institute of Technology

(Dated: January 28, 2020)

We have measured the magnetic susceptibility of single crystal samples of non-hydrated Na_xCoO_2 ($x \sim 0.75, 0.67, 0.5$, and 0.3) and hydrated $\text{Na}_{0.3}\text{CoO}_2\cdot y\text{H}_2\text{O}$ ($y \sim 0, 0.6, 1.3$). Our measurements reveal considerable anisotropy between the susceptibilities with $\text{H} \parallel \text{c}$ and $\text{H} \parallel \text{ab}$. The derived anisotropic g-factor ratio (g_{ab}/g_c) decreases significantly as the composition is changed from the Curie-Weiss metal with $x = 0.75$ to the paramagnetic metal with $x = 0.3$. Fully hydrated $\text{Na}_{0.3}\text{CoO}_2\cdot 1.3\text{H}_2\text{O}$ samples have a larger susceptibility than non-hydrated $\text{Na}_{0.3}\text{CoO}_2$ samples, as well as a higher degree of anisotropy. In addition, the fully hydrated compound contains a small additional fraction of anisotropic localized spins.

PACS numbers: 74.25 Ha, 74.70.Dd, 75.20.Hr, 75.30.Gw, 75.30.Cr

I. INTRODUCTION

The discovery of superconductivity below $T \sim 4.5$ K in $\text{Na}_{0.3}\text{CoO}_2\cdot 1.4\text{H}_2\text{O}$ has engendered much interest in the family of $\text{Na}_x\text{CoO}_2\cdot y\text{H}_2\text{O}$ compounds.¹ Recent research has focused on understanding the mechanism for superconductivity in the new hydrated superconductor. Examining the bulk properties of $\text{Na}_x\text{CoO}_2\cdot y\text{H}_2\text{O}$ as a function of x and y is a crucial step toward explaining the intriguing physics found on the phase diagram, such as the anomalously large thermoelectric power and superconductivity.² Initial reports suggest that the Na_xCoO_2 material crosses over from a Curie-Weiss metal ($x > 0.5$) to a paramagnetic metal ($x < 0.5$), separated by a charge-ordered insulator.³ Spin entropy is believed to play an important role in the enhanced thermopower in $\text{Na}_{0.68}\text{CoO}_2$.⁴ Based on density-functional calculations, weak itinerant ferromagnetic fluctuations have been suggested to compete with weak antiferromagnetism for $x = 0.3$ to $x = 0.7$.⁵ Further progress can be made on the experimental side by carefully studying the evolution of the spin behavior as the Na concentration is decreased from $x=0.75$ to 0.3 . In this paper, we present a systematic study of the anisotropic magnetic susceptibility using high-quality single crystals with well controlled stoichiometry produced by an electrochemical de-intercalation method.⁶

II. EXPERIMENTAL

Single crystals of $\text{Na}_{0.75}\text{CoO}_2$ were grown using a floating-zone method as described previously.⁶ After an additional electrochemical de-intercalation procedure, samples were produced with the final Na concentrations of $x = 0.75, 0.67, 0.5$ and 0.3 , as confirmed by Electron Microprobe Analysis.⁷

A fully hydrated $\text{Na}_{0.3}\text{CoO}_2\cdot 1.3\text{H}_2\text{O}$ crystal was prepared by enclosing a non-hydrated $\text{Na}_{0.3}\text{CoO}_2$ crystal within a water vapor saturated environment for ~ 4 months. After this period of hydration, the crystal consisted of a single phase with a c-axis lattice constant of $\sim 19.6\text{\AA}$ and with a superconducting transition temperature near ~ 4.2 K. Partially hydrated $\text{Na}_{0.3}\text{CoO}_2\cdot 0.6\text{H}_2\text{O}$ samples and a fully dehydrated $\text{Na}_{0.3}\text{CoO}_2$ samples were obtained by driving water out by annealing at temperatures of 120 °C and 220 °C, respectively, for 15 hours. Except for a small fraction of a Co_3O_4 impurity phase generated in the fully dehydrated crystal, the partially hydrated and fully dehydrated phases have c-axis lattice constants of $\sim 13.8\text{\AA}$ and 11.2\AA , respectively, which are in agreement with previously reported values of $\text{Na}_{0.3}\text{CoO}_2\cdot 0.6\text{H}_2\text{O}$ and $\text{Na}_{0.3}\text{CoO}_2$.⁸ In principal, the fully dehydrated (FD) phase should be identical to the original non-hydrated phase. Powder x-ray diffraction results confirm that the two phases share the same primary powder peaks; however, the FD sample contains a somewhat higher degree of defects which we will discuss further below.

Measurements of the magnetic susceptibility were performed using a Quantum Design MPMS-XL SQUID magnetometer. All data were measured under a magnetic field of 1 Tesla through both zero cooled and zero-field cooled sequences. Slightly hysteretic behavior was observed for the $x = 0.75$ sample near temperatures of ~ 22 K and ~ 320 K.⁹ Since the focus of this paper is not on the hysteretic behavior, all of the data presented are based on the zero-field cooled results. A background correction to the susceptibility has been made on the crystals with $x = 0.67$ and 0.3 . The source of this background is likely due to a small amount of CoO impurities (about a 7 % mass fraction) imbedded between the grain boundaries of the particular starting boule of $\text{Na}_{0.75}\text{CoO}_2$. The CoO correction was implemented as to minimize the contribution from the antiferromagnetic transition ($T_N \sim 290$ K)

of CoO, while maintaining the same magnitude of the susceptibility as a powder sample of the same stoichiometry.⁷ No correction was applied to the $\text{Na}_{0.75}\text{CoO}_2$ and $\text{Na}_{0.5}\text{CoO}_2$ crystals, where no anomaly at $T \sim 290$ K is found and the powder averaged data agrees with the data from stoichiometric polycrystalline samples. We note, however, there is a broad maximum near ~ 275 K for the $\text{Na}_{0.67}\text{CoO}_2$ crystal, which may be intrinsic, as this is also reported by others.⁹ One additional crystal of $x \sim 0.7$, grown with the flux-method, is presented together in Table 1 for comparison purposes.

III. RESULTS AND DISCUSSION

1. Magnetic susceptibility of non-hydrated Na_xCoO_2

The complete magnetic susceptibility data of Na_xCoO_2 ($x = 0.3, 0.5, 0.67$, and 0.75) are shown in Fig. 1, where a magnetic field of 1 Tesla was applied parallel to both the ab - and c -directions. The susceptibility is composed of temperature-independent Van Vleck paramagnetic (χ_{vv}) and core diamagnetic (χ_{core}) contributions, and also a temperature-dependent term, $\chi_e(T)$, which represents contributions from either localized spins (χ_s) or the spin response of delocalized electrons (Pauli paramagnetism χ_{pauli}),

$$\chi(T) = \chi_{core} + \chi_{vv} + \chi_e(T).$$

Curie-Weiss-like behavior is observed for $x > 0.5$, but samples with $x < 0.5$ show a monotonic increase of χ with increasing temperatures. Our results, when powder-averaged, agree with the published powder measurements on samples prepared using chemical Br_2 de-intercalation.³

Our single crystal results yield additional information on the spin anisotropy. In Fig. 2, plots of χ_{ab} versus χ_c are shown for all crystals for temperatures between 50 and 250 K. The χ_{ab} versus χ_c curve shows a remarkably linear relationship for all x . We can analyze this data by writing the total susceptibility as a sum of a temperature-independent and a temperature-dependent term: $\chi^{ab,c} = \chi_o^{ab,c} + \chi_e^{ab,c}(T)$. We then assume that the temperature-dependent term can be written in the form $\chi_e^{ab,c}(T) = (g_{ab,c})^2 f(T)$. Hence, in this model, the anisotropy of the spin susceptibility χ_e results from an anisotropic g-factor. Note that the g-factor for localized spins is related to the spin-orbit coupling (which may be anisotropic), whereas the effective g-factor for delocalized electrons is related to the coupling between the applied field and the total angular momentum of the system. This leads to the following relation between χ_{ab} and χ_c :

$$\chi_{ab} = (g_{ab}/g_c)^2 \chi_c + [\chi_o^{ab} - (g_{ab}/g_c)^2 \chi_o^c].$$

As evident in this equation, the fitted slope of the data

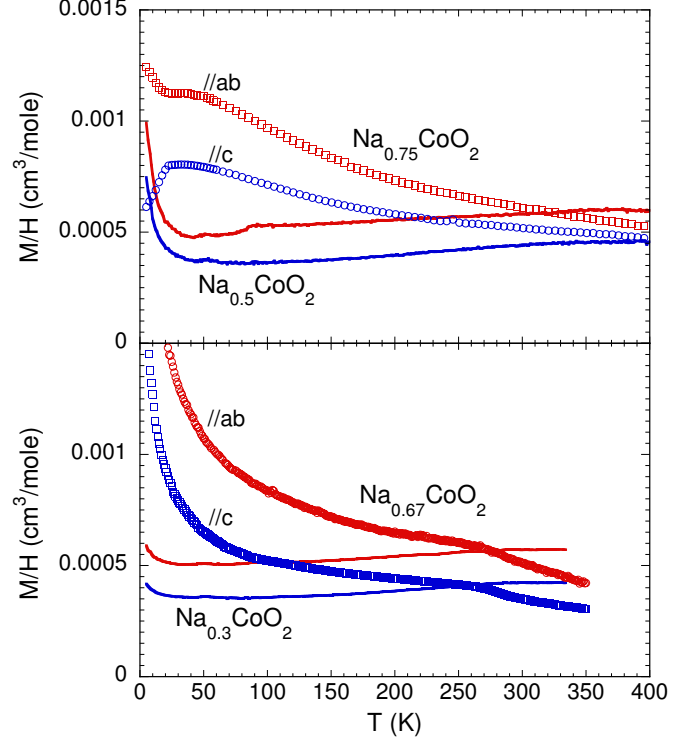


FIG. 1: Magnetic susceptibilities of Na_xCoO_2 ($x = 0.75, 0.67, 0.5$, and 0.3) under a magnetic field of 1 Tesla. The red and blue symbols are for the magnetic field applied along the ab - and c -directions, respectively.

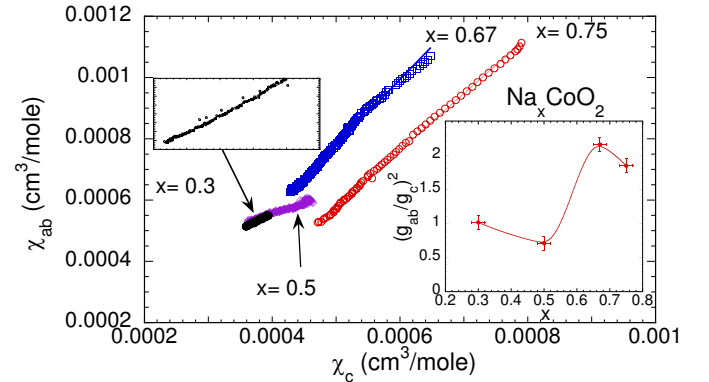


FIG. 2: χ_{ab} versus χ_c for Na_xCoO_2 with $x = 0.75, 0.67, 0.5$ and 0.3 . The inset shows the fitted slope which corresponds to $(g_{ab}/g_c)^2$ as described in the text.

in Fig. 2 corresponds to the ratio $(g_{ab}/g_c)^2$. This ratio is plotted as a function of x in the inset of Fig. 2. The sample with $x = 0.67$ has the largest anisotropy of $g_{ab}/g_c \sim 1.45$, whereas the sample with $x = 0.3$ is nearly isotropic. In the case where localized moments exist on the Co ions, the t_{2g} orbitals are more than half-filled and a level splitting exists as a result of the CoO_6 octahedral distortion.¹⁰ Hence, a g-factor larger than 2 is expected. Assuming $g_c = 2$, then g_{ab} would be as high as 2.68 for

TABLE I: Curie-Weiss fitting parameters for Na_xCoO_2

		$x=0.75$	$x=0.70^a$	$x=0.67$	$x=0.50^b$
ab	χ_\circ	.000187	.000268	.000375	.000290
ab	C	.181	.145	.0677	.00325
ab	θ	-130	-103	-46.9	-1.94
c	χ_\circ	.000326	.000223	.000358	.000350
c	C	.0751	.0665	.0183	.00481
c	θ	-93	-64.5	-12.0	-2.33
Powder	χ_\circ	.000231	.000267	.000356	.000295
Powder	C	.147	.112	.0554	.00520
Powder	θ	-125	-87.8	-46.9	-3.21

^aflux grown^bfitted 5-30K

$x=0.75$. One sees a clear difference in the spin anisotropy for samples with $x>0.5$ and those with $x<0.5$. This behavior further highlights the unusual metallic state which exists in the phase diagram for $x>0.5$.

For the samples with $x = 0.67$ and 0.75 , we fit the high-temperature susceptibility to a Curie-Weiss law, $\chi = \chi_\circ + C/T$ in the range $T = 50 - 250$ K. The samples with $x = 0.5$ and 0.3 have a different temperature dependence in this temperature range. However, there is a clear Curie tail below $T \sim 30$ K for $x = 0.5$, and this has been fit for temperatures between 5 and 30 K. The fitting parameters for both field orientations, as well as the powder average, are shown in Table 1. For comparison purposes, an additional set of data from a crystal with $x = 0.7$ grown with the flux method is also shown. The results of the fits have a small dependence on the choice of the temperature range selected. Overall, however, the fits appear to converge with an error within 15%. The temperature-independent value for χ_\circ also agrees well with the estimate of the orbital contribution ($\sim 2 \times 10^{-4}$ cm³/mole) from Knight shift analysis of ⁵⁹Co NMR.¹¹ Assuming that the only pair of split energy levels is between the a_{1g} and E_g levels within the t_{2g} band, and that χ_{pauli} is negligible, the large value for χ_{vv} indicates the two low lying crystal-field states of the Co⁴⁺ ions are close in energy.

In view of the many conflicting results regarding the Curie-Weiss fit of the susceptibility of $\text{Na}_{0.75}\text{CoO}_2$, we have examined the validity of our fits using five different batches of $\text{Na}_{0.75}\text{CoO}_2$ powder, and using different temperature ranges for the fit. All Curie constants fall reliably near 0.149 ± 0.025 K-cm³/mole. The fitted values for the powder average of the single crystal with $x = 0.75$ has a Curie constant ~ 0.147 K-cm³/mole, $\chi_\circ \sim 2 \times 10^{-4}$ cm³/mole, and Weiss temperature ~ -125 K. Using the previously derived ratio $(g_{ab}/g_c)^2 \sim 1.8$ and assuming $g_c \sim 2$, the powder average $g^2 = (2/3 * g_{ab}^2 + 1/3 * g_c^2)$ is calculated to be 6.12. Assuming all electrons in the t_{2g}^5 orbitals are in the low spin state ($s = 1/2$), the fitted Curie constant indicates that $26 \pm 2\%$ of the Co ions have a localized spin. Hence, nearly all of the Co⁴⁺ ions in $\text{Na}_{0.75}\text{CoO}_2$ have a localized spin of 1/2. Alternatively,

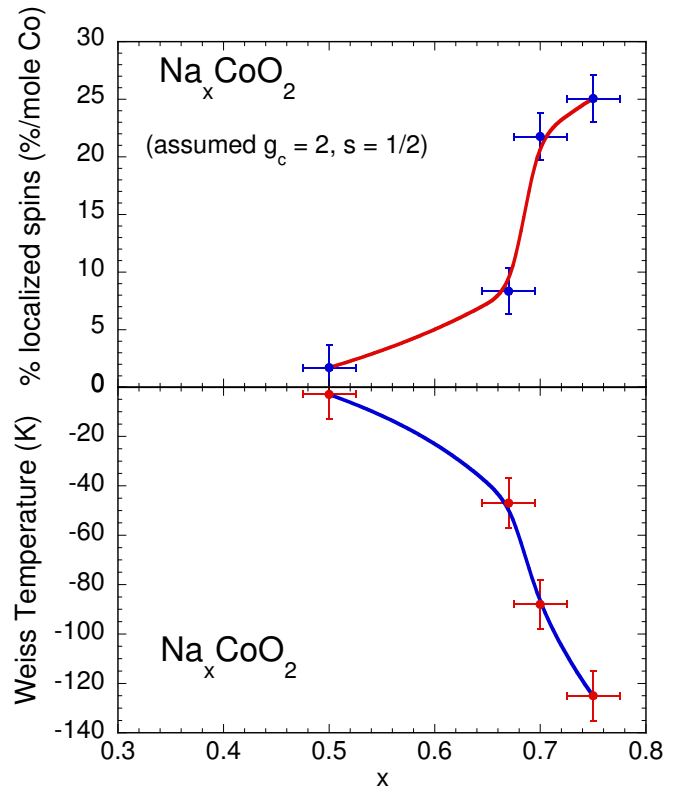


FIG. 3: Top panel: fraction of localized spins per mole Co versus x . Bottom panel: the Weiss temperature versus x . The lines serve as guides for the eye.

the value of the Curie constant is consistent with an interpretation that the effective local moment is $\sim 1.1\mu_B$ if averaged over all of the Co ions. In either interpretation, the coexistence of localized spins and metallic behavior in this compound remains an intriguing issue to understand. It is likely related to the presence of strong correlations, which may also give rise to other unusual properties such as the signatures of mass enhancement.⁶

Using the ratios for $(g_{ab}/g_c)^2$ values derived in Fig. 2 and the Curie constants shown in Table 1, we have analyzed the susceptibility data for $x = 0.7$, 0.67 , and 0.5 in a similar manner. The results are summarized in Fig. 3, where we plot the fraction of localized spins per mole of Co and the Weiss temperatures as a function of x . We find that while almost all of the Co⁴⁺ spins are localized for $x = 0.75$, the fraction of localized spins drops precipitously below $x = 0.67$. Local moment behavior disappears almost entirely for $x = 0.5$. In parallel with the loss of local moments, the magnitude of the Weiss temperature decreases drastically with decreasing x . The Weiss temperature of about -125 K for $x = 0.75$ suggests antiferromagnetic (AF) correlations between Co⁴⁺ spins. There is a clear reduction in the strength of the AF correlations as x decreases to $x = 0.5$ (where the Weiss temperature is about -3 K). These results demonstrate that de-intercalating Na from $\text{Na}_{0.75}\text{CoO}_2$ modifies the

spin system from one described by localized spins to one described by delocalized spins with weaker magnetic coupling.

2. Magnetic susceptibility of $\text{Na}_{0.3}\text{CoO}_2\cdot y\text{H}_2\text{O}$

The magnetic susceptibilities of single crystal samples of $\text{Na}_{0.3}\text{CoO}_2\cdot y\text{H}_2\text{O}$ (with $y \sim 0, 0.6, 1.3$) are shown in Fig. 4. These data were taken on a single sample which originally had the composition $\text{Na}_{0.3}\text{CoO}_2\cdot 1.3\text{H}_2\text{O}$ and was subsequently annealed to reduce the water content to $y=0.6$ and then $y=0$. All three samples show nearly temperature-independent susceptibilities with weak Curie-like behavior developing below $\sim 200\text{K}$. As water is driven out, the anisotropy of the susceptibility is reduced, and, at the same time, the Curie behavior becomes enhanced. In addition, the fully dehydrated crystal is observed to have a small Co_3O_4 impurity phase, likely caused by the dehydration process due to partial decomposition. By fitting the susceptibility above $T=50\text{ K}$ for the fully dehydrated crystal to a Curie law, we find that the Curie constant is isotropic and corresponds to about $\sim 6\%$ isolated Co^{4+} ions. This term has been subtracted from the data in the bottom panel of Fig. 4 since it behaves like a paramagnetic impurity. Indeed the Curie corrected susceptibility data for this fully dehydrated $\text{Na}_{0.3}\text{CoO}_2$ crystal are very similar to the data for the non-hydrated $\text{Na}_{0.3}\text{CoO}_2$ crystal shown in Fig. 1 (which do not require this correction). There is a cusp in the susceptibility near $T \sim 42\text{ K}$ for both the fully hydrated and partially hydrated crystal, which we will discuss further below.

In Fig. 5, we plot χ_{ab} versus χ_c , which again has a remarkably linear dependence. An anisotropic Curie-Weiss law $\chi_o + C/T$ has been used to fit both directions. The complete list of fit parameters is shown in Table 2. Both C_{ab}/C_c and $(g_{ab}/g_c)^2$ are plotted in the inset of Fig. 5. We find that the ratio $(g_{ab}/g_c)^2$ is greater than 1 for both the fully hydrated and partially hydrated samples. This indicates that the paramagnetic impurities which give rise to the Curie-Weiss behavior are not isotropic, but are strongly affected by the anisotropic orbital environment. Such Curie-Weiss behavior is absent in the non-hydrated $\text{Na}_{0.3}\text{CoO}_2$ crystal shown previously in Fig. 1. The Curie constant for the fully hydrated $\text{Na}_{0.3}\text{CoO}_2\cdot 1.3\text{H}_2\text{O}$ crystal ($\sim 0.0036\text{ K}\cdot\text{cm}^3/\text{mole}$) suggests about $\sim 1\%$ of the spins ($s = 1/2$ and $g^2 \sim 6.9$) in the system are localized. These localized spins may be related to defects formed during hydration as a result of local structure deformation. However, their origin remains a topic for further investigation. Such enhanced Curie-like behavior has also been reported in powder sample prepared with the chemical Br_2 de-intercalation method as well.¹²

Two major differences are made apparent by comparing the susceptibility data of the fully hydrated (FH) $\text{Na}_{0.3}\text{CoO}_2\cdot 1.3\text{H}_2\text{O}$ and non-hydrated $\text{Na}_{0.3}\text{CoO}_2$ crystals displayed in Fig. 6. First, the FH sample has a

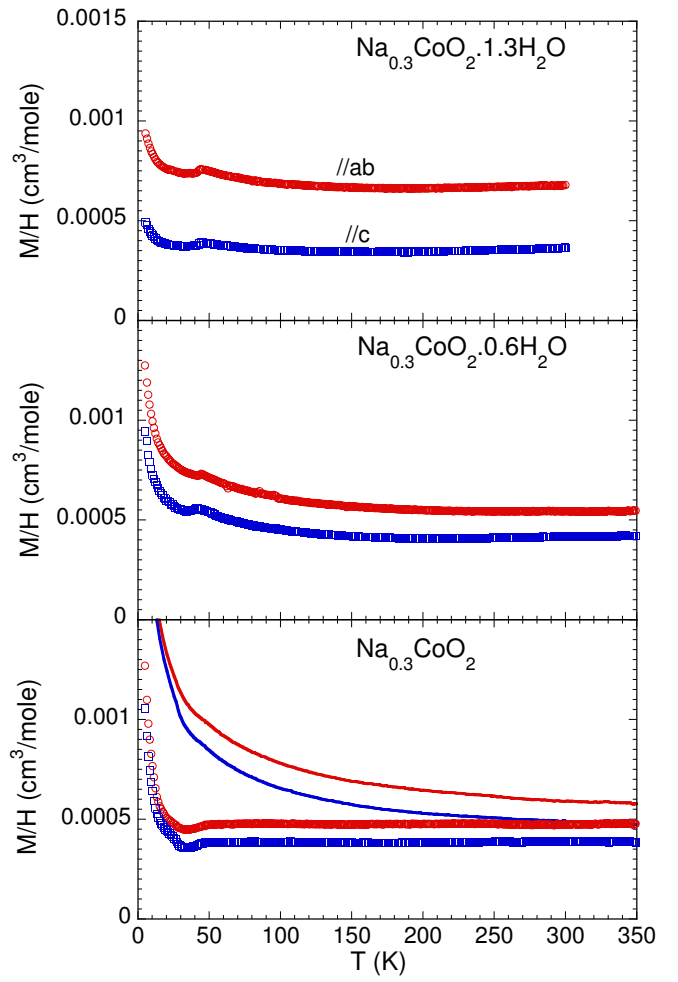


FIG. 4: Magnetic susceptibilities of $\text{Na}_{0.3}\text{CoO}_2\cdot y\text{H}_2\text{O}$ ($y = 0, 0.6$, and 1.3) under a magnetic field of 1 Tesla. The red and blue symbols are for field applied along the ab and c directions respectively. The third panel for $\text{Na}_{0.3}\text{CoO}_2$ shows data both before (lines) and after (symbols) a Curie tail was subtracted.

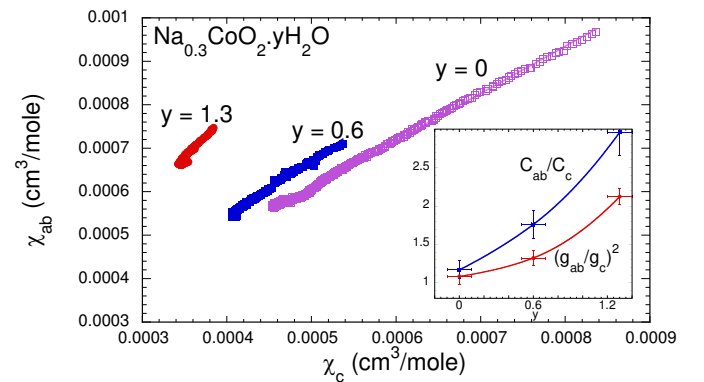


FIG. 5: χ_{ab} versus χ_c for $\text{Na}_{0.3}\text{CoO}_2\cdot y\text{H}_2\text{O}$ with $y = 0, 0.6$ and 1.3 . The inset shows the fitted slope which corresponds to $(g_{ab}/g_c)^2$ and Curie constant ratio (C_{ab}/C_c) as described in the text.

TABLE II: Curie-Weiss fitting parameters for $\text{Na}_{0.3}\text{CoO}_2 \cdot y\text{H}_2\text{O}$

		$y=1.3$	$y=1.3^a$	$y=0.6$	$y=0.6^a$	$y=0$	$y=0^a$
ab	χ_o	.000634	.000631	.000472	.000571	.000476	.000667
ab	C	.00474	.00333	.0167	.00548	.0385	.0157
ab	θ	10.2	-6.22	-20.6	-2.71	-26.7	-3.51
c	χ_o	.000334	.000334	.000360	.000425	.000383	.000578
c	C	.00160	.00106	.00954	.00384	.0327	.0162
c	θ	21.2	-1.24	-4.12	-2.29	-20.4	-4.12
Powder	χ_o	.000533	.000559	.000444	.000539	.000441	.000638
Powder	C	.00363	.00168	.0119	.00456	.0380	.0158
Powder	θ	14.0	-1.80	-5.93	-2.18	-27.6	-3.70

^afitted 5-20K

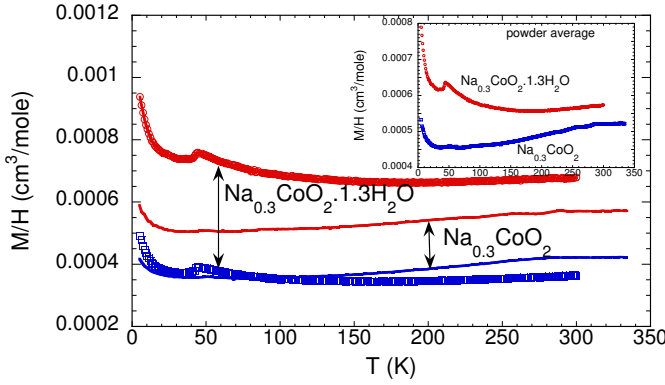


FIG. 6: Magnetic susceptibilities of non-hydrated $\text{Na}_{0.3}\text{CoO}_2$ and fully hydrated $\text{Na}_{0.3}\text{CoO}_2 \cdot 1.3\text{H}_2\text{O}$. The powder average is shown in the inset.

larger anisotropy. Second, the FH sample has a larger total susceptibility, as further confirmed by the powder average data in the inset of Fig. 6. The larger anisotropy likely results from the structural changes of the CoO layers caused by the hydration. The higher susceptibility may result from a change in χ_{vv} or χ_{pauli} , although we can not separate these two contributions independently. We note that NMR measurements show that the ^{59}Co Knight shift is significantly enhanced upon hydration,¹¹ consistent with our findings. If the susceptibility increase is dominated by χ_{vv} , a smaller t_{2g} splitting would indicate a less distorted CoO_6 octahedra. However, the neutron powder results of Lynn *et al.* indicate that a fully hydrated sample actually has a larger octahedral distortion compared with a non-hydrated one.¹³ On the other hand, if χ_{pauli} is dominant, this implies that the fully hydrated sample has a higher density of states at the Fermi level. This is consistent with our preliminary specific heat data, which show that a fully hydrated crystal has a higher value for the Sommerfeld constant than a fully dehydrated one.¹⁴. The Na_xCoO_2 compositions with $x = 0.3$ and 0.5 have close values for the open circuit potential achieved during the electrochemical de-intercalation process.⁷ We compare these two phases in Fig. 7 and find the susceptibilities of these two phases are almost identi-

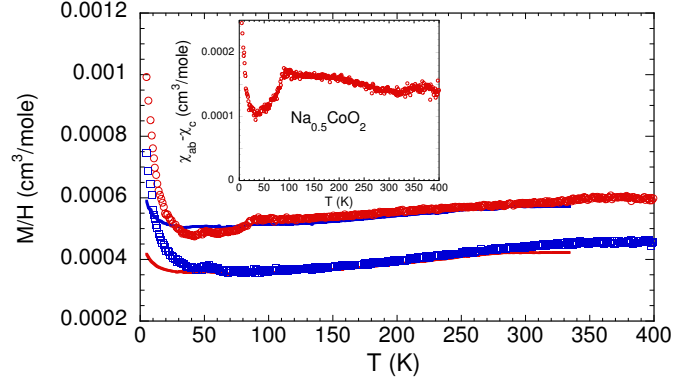


FIG. 7: Magnetic susceptibilities of $\text{Na}_{0.5}\text{CoO}_2$ and $\text{Na}_{0.3}\text{CoO}_2$, the former is shown in symbols. The inset shows the difference ($\chi_{ab} - \chi_c$) for $\text{Na}_{0.5}\text{CoO}_2$

cal (within the errors) above $\sim 100\text{K}$, similar to that reported previously in powder samples.³ We find that our non-hydrated $\text{Na}_{0.3}\text{CoO}_2$ sample develops small anomalies near $T=53\text{ K}$ and $T=88\text{ K}$, after the crystal was stored in air for more than 6 months. This suggests that some degree of Na phase separation occurs over long time scales. In our $\text{Na}_{0.5}\text{CoO}_2$ sample, the susceptibility cusp at 53K is nearly isotropic, whereas the one near 88K is clearly anisotropic as shown in the inset.

Finally, we remark upon the 42 K anomaly observed in both fully hydrated $\text{Na}_{0.3}\text{CoO}_2 \cdot 1.3\text{H}_2\text{O}$ and partially hydrated $\text{Na}_{0.3}\text{CoO}_2 \cdot 0.6\text{H}_2\text{O}$ crystals (shown previously in Fig. 4). This anomaly is much weaker or absent in the fully dehydrated and non-hydrated $\text{Na}_{0.3}\text{CoO}_2$ crystals. Hence, we conclude that the anomaly results from the hydration process. However, it is not clear at this point if this reflects the intrinsic behavior of the hydrated sample, or if it originates from an impurity phase. We note that the 42 K anomaly does not exist in fully hydrated powder samples, irrespective of chemical or electrochemical de-intercalation. It is therefore tempting to assign the 42 K anomaly to the existence of a Co_3O_4 impurity, especially since the bulk AF transition temperature of Co_3O_4 occurs around $\sim 33\text{K}$. However, hysteretic behavior is observed near 42 K (not shown), which is not

expected from a Co_3O_4 impurity phase. Sasaki et al. have also reported a 42 K anomaly in hydrated single crystal samples.¹⁵ They proposed that it originates from residual oxygen on the surface of the crystal. However, if this is only a surface effect, powder samples should show a more pronounced 42 K anomaly under the same treatment. Unlike studies on K_xCoO_2 powder samples, where a Co_3O_4 inclusion can be reliably subtracted from the total susceptibility,¹⁶ we cannot completely eliminate the anomaly near 42 K with a simple subtraction of a Co_3O_4 ($T_N \sim 33\text{K}$) impurity phase.

IV. CONCLUSIONS

We have presented a systematic study of the magnetic susceptibility of $\text{Na}_x\text{CoO}_2\cdot y\text{H}_2\text{O}$ (with $0.3 < x < 0.75$ and $y \sim 0, 0.6$ and 1.3) using high-quality single crystal samples with well controlled Na contents. For non-hydrated samples, we find that the derived anisotropic g-factor ratio (g_{ab}/g_c) decreases significantly as the composition is changed from the Curie-Weiss metal with $x = 0.75$ to the paramagnetic metal with $x = 0.3$. We confirm that a model of localized Co^{4+}

spins describes the spin susceptibility of $\text{Na}_{0.75}\text{CoO}_2$. However, the fraction of localized spins decreases precipitously upon de-intercalation. For the composition with $x=0.3$, the anisotropy in the susceptibility becomes more pronounced with increasing hydration. In addition, the magnitude of the susceptibility is larger in fully hydrated $\text{Na}_{0.3}\text{CoO}_2\cdot 1.3\text{H}_2\text{O}$ than in non-hydrated $\text{Na}_{0.3}\text{CoO}_2$. The hydrated crystals also contain a small additional fraction of anisotropic localized spins. These results provide a big picture view of how the spin behavior evolves with changing Na content and water content.

Acknowledgments

We thank Patrick Lee and Takashi Imai for many insightful discussions. This work was supported primarily by the MRSEC Program of the National Science Foundation under award number DMR-02-13282. J. H. Cho was partially supported by Grant No. (R01-2000-000-00029-0) from the Basic Research Program of the Korea Science and Engineering Foundation.

^{*} On leave from Physics Department, Pusan National University, Korea.

¹ K. Takada, H. Sakurai, E. Takayama-Muromachi, F. Izumi, R. Dilanian, and T. Sasaki, *Nature* **422**, 53 (2003).

² I. Terasaki, Y. Sasago, and K. Uchinokura, *Phys. Rev. B* **56**, R12685 (1997).

³ M. L. Foo, Y. Wang, S. Watauchi, H. W. Zandbergen, T. He, R. J. Cava, and N. P. Ong, *cond-mat/0312174*.

⁴ Y. Wang, N. S. Rogado, R. J. Cava, and N. P. Ong, *Nature* **423**, 425 (2003).

⁵ D. J. Singh, *Phys. Rev. B* **68**, 020503 (2003).

⁶ F. C. Chou, J. H. Cho, P. A. Lee, E. T. Abel, K. Matan, and Y. S. Lee (2004), to be published in *Phys. Rev. Lett.*

⁷ F. C. Chou and *et. al.*, unpublished.

⁸ M. L. Foo and *et al*, *Sol. St. Comm.* **127**, 33 (2003).

⁹ D. Prakhakaran, A. T. Boothroyd, R. Coldea, and L. M. Helme, *cond-mat/0312493*.

¹⁰ Q. Wang, D. Lee, and P. A. Lee, *cond-mat/0304377*.

¹¹ T. Imai and *et al.*, unpublished.

¹² H. Sakurai, K. Takada, F. Izumi, D. A. Dilanian, T. Sasaki, and E. Takayama-Muromachi, *cond-mat/0310717*.

¹³ J. W. Lynn, Q. Huang, C. M. Brown, V. L. Miller, M. L. Foo, R. E. Schaak, C. Y. Jones, E. A. Mackey, and R. J. Cava, *Phys. Rev. B* **68**, 214516 (2003).

¹⁴ J. H. Cho and *et al*, unpublished.

¹⁵ T. Sasaki, P. Badica, N. Yoneyama, K. Yamada, K. Togano, and N. Kobayashi, *cond-mat/0402355*.

¹⁶ S. Nakamura, J. Otake, N. Yonezawa, and S. Iida, *J. Phys. Soc. Jpn.* **65**, 358 (1996).